Available online at www.sciencedirect.com
SCIENCE DIRECT®
PERGAMON
International Journal of Heat and Mass Transfer 46 (2003) 3661–3672
International Journal of HEAT and MASS TRANSFER
www.elsevier.com/locate/ijhmt

Natural convection around a horizontal heated cylinder: The effects of vertical confinement

Mohamed A. Atmane [a,*], Victor S.S. Chan [b], Darina B. Murray [b]

[a] *Applied Physics Laboratory, 1013, 40th Street NE, Seattle, WA 98105, USA*
[b] *Mechanical Engineering Department, Parsons Building, Trinity College, Dublin, D2, Ireland*

Received 5 August 2002; received in revised form 8 March 2003

Abstract

The effect of vertical confinement on the natural convection flow and heat transfer around a horizontal heated cylinder is investigated. The flow characteristics and the time-resolved heat transfer have been measured respectively above and around the cylinder. It is shown that the primary effect of the vertical confinement is an increase in heat flux on the upper part of the cylinder for given separation distances between the cylinder and the fluid boundary. This increase is shown to be related to the large-scale oscillation of the thermal plume. The relationship between the flow pattern and the heat transfer characteristics at the cylinder surface is studied and the origin of the oscillation discussed.

1. Introduction

Natural convection around a circular horizontal heated cylinder has been extensively studied for the case in which the cylinder is suspended in an infinite medium. Correlations giving the Nusselt number as a function of the Rayleigh number have been proposed for a wide range of Rayleigh numbers, as summarized by Kitamura et al. [1], for example. When the fluid medium around the cylinder is vertically or horizontally confined, the natural convection can be affected dramatically. For instance, Karim et al. [2] have experimentally demonstrated the influence of horizontal confinement on heat transfer around a cylinder for Rayleigh numbers ranging from 10^3 to 10^5. These authors found that the heat flux around the cylinder increases with decreasing distance between the cylinder and the enclosure wall. Cesini et al. [3] carried out experiments similar to those of Karim et al. [2] but found that the heat flux from the cylinder reached a maximum for an optimal wall-to-wall distance of 2.9 times the cylinder diameter. Their numerical simulations showed a similar trend. This result was attributed to changes in the heat transfer mode from convective to conductive. An interesting observation made by Cesini et al. [3] was that for Rayleigh numbers higher than 10^5, oscillations of the heat flux at the surface of the cylinder appeared. However, the origin of these oscillations was not investigated.

The case of vertical confinement is not as well documented as the horizontal one. A vertically confined natural convection flow around a horizontal cylinder has many practical applications, ranging from the cooling of electronic components to the transport of oil through pipelines below the water surface or at the sea floor. Vertical confinement can produce a complex combination of effects. Koizumi and Hosokawa [4] investigated a natural convection flow around a cylinder, vertically confined by a ceiling, and reported on chaotic and oscillatory movements of the air above the cylinder. These authors gave a classification of the nature of the flow above the cylinder, the classification depending on the Rayleigh number and on the distance separating the ceiling from the cylinder. Their experiments were carried out with both conductive and adiabatic ceilings. In contrast to the horizontal confinement case, it is not clear what mechanisms are involved in the heat transfer enhancement.

* Corresponding author. Address: Civil Engineering Department, University of Alberta, Edmonton, AB, Canada T6G 2G7. Tel.: +1-780-492-3188; fax: +1-780-492-0249.
E-mail address: matmane@civil.ualberta.ca (M.A. Atmane).

0017-9310/03/$ - see front matter
doi:10.1016/S0017-9310(03)00154-6

Nomenclature

A	velocity amplitude computed from the horizontal and vertical components (in mm/s)	Pr	Prandtl number
D	diameter of the cylinder	Ra	Rayleigh number
H	distance between the top of the cylinder and the free surface	U	horizontal component of the velocity (in mm/s)
Nu	Nusselt number	W	vertical component of the velocity (in mm/s)
		β	angular position of the sensor in °

The objective of the present work is to investigate the dynamics of the plume above a heated horizontal cylinder, mounted in a water tank and vertically confined by the water free surface. Thus, we expect to find a relationship between the dynamics of the plume and the increase in heat transfer over the top of the cylinder. The work involves both investigation of heat transfer around the cylinder and measurement of the hydrodynamics field above it. Experiments are carried out with the focus on identifying the effect of the free water surface on heat transfer at the heated cylinder surface. In contrast to Koizumi and Hosokawa [4], a free surface was chosen as a boundary in the present work. This choice facilitates generalization of the observation of oscillatory motions of the plume and provides a complementary database for the case of an adiabatic boundary, a case for which the results of Koizumi and Hosokawa are limited.

The Digital Particle Image Velocimetry (DPIV) technique, in which the velocity field is resolved in space and time, is used to clarify the behavior of the thermal plume above the cylinder. In addition to the quantitative information it gives on the velocity amplitudes, the technique also provides a qualitative insight into the flow characteristics above the cylinder. Such a description has not been reported before in the literature.

The work is divided into three parts. Firstly, the heat transfer characteristics around the cylinder are presented for different cylinder-to-wall temperature differences and for different separation distances between the cylinder and the water surface. In order to extend the range of Rayleigh numbers for the heat flux sensor calibration, air was used as a fluid medium during some of these experiments. In the second part of this study, the hydrodynamics is thoroughly investigated using DPIV. The main characteristics of the natural convection flow above the cylinder are presented and compared for different water surface elevations. Some features of the oscillatory movement above the cylinder are identified and the conditions for oscillation to occur are documented. In the last section, we explore the time varying heat flux and surface temperature characteristics and demonstrate the close relationship that exists between the velocity field in the fluid and the heat transfer characteristics at the wall of the cylinder.

2. Experimental rig and procedures

The experiments have been conducted in an aluminum tank, 700 mm high, 600 mm long and 300 mm wide. Glass windows have been fitted on the sides of the tank to allow for visual access to the flow. A plain horizontal cylinder made of copper is fitted between two of the glass windows, at 300 mm from the bottom of the tank. The cylinder is 270 mm long, has an external diameter $D = 30$ mm and is internally heated using two cartridge heaters (0.5 kW each). The cylinder is equipped with a heat flux sensor (Micro-Foil™ heat flux sensor model 27036-1-RdF). In addition to measuring the surface heat flux, the sensor also measures the cylinder surface temperature. The manufacturer specifies a response time of 50 Hz. This sensor is similar to that used by Murray [5]. A schematic of the tank, the cylinder and the DPIV system is shown in Fig. 1a and b.

In the first part of this work, both air and water have been used as fluid media in order to recalibrate the heat flux sensor. In the second and third parts, water is used as the test fluid. In the latter case, the water mass in the tank was replaced by fresh water at ambient temperature every 15 min, to avoid the effects of temperature drift over large time scales. This procedure allowed us to limit the increase in the average water temperature to approximately 2 °C throughout a given run typically 60 min long. All measurements were performed when the natural convection flow reached a pseudo-steady state during which the variation of the average heat flux at a given point on the cylinder was not significant (i.e. the time-averaged heat flux may vary significantly with position but not with time).

The factor H/D is the first control parameter of the experiments (H is the distance between the water surface and the top of the cylinder and D is the diameter of the cylinder). Three water levels H will be investigated in this study: $H = D/2$, $H = D$ and $H = 3D$. These levels were selected following preliminary experiments that showed that for water levels above $H = 3D$, heat transfer around the cylinder and the natural convection hydrodynamics were not affected by the water surface. The second control parameter (ΔT) is the difference between the cylinder surface temperature (T_s) and the

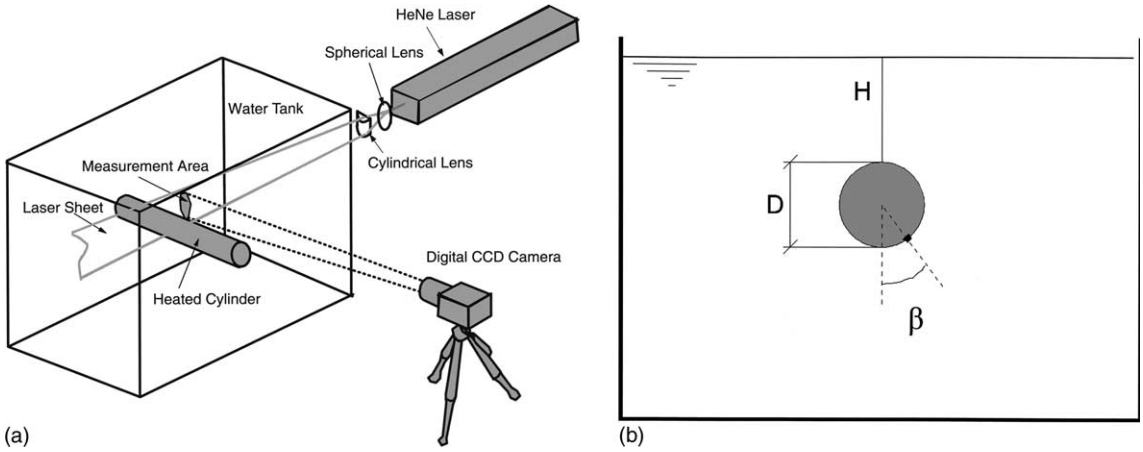

Fig. 1. (a) Schematic representation of the experimental set-up. (b) Side view of the tank.

water bulk (T_∞). The water bulk temperature is measured close to the tank wall, at the same horizontal level as the cylinder. This second parameter dictates the natural convection flow regime and is generally expressed in the form of the Rayleigh number defined as:

$$Ra = BgD^3\Delta TPr/\upsilon^2$$

where B is the volumetric thermal expansion coefficient of the fluid, g the gravitational constant, Pr the Prandtl number and υ the kinematic viscosity of water. All parameters are evaluated at the fluid 'film' temperature defined as:

$$T_f = \frac{T_s + T_\infty}{2}$$

In the work reported here, the maximum Rayleigh number was of the order of 10^7, meaning that the flow is nominally still laminar.

The hydrodynamics of the flow is investigated using a DPIV system. It consists of a Spectra Physics 32 mW continuous He/Ne laser, a laser sheet generator, a Dalsa CA-D6-0256 high speed CCD camera and a personal computer equipped with two separate frame grabbers. The low velocity amplitudes evaluated during natural convection made the use of a continuous laser sufficient. Neutrally buoyant polyamid particles with a nominal size of 20 μm and a specific gravity of 1.02 were used for seeding the water. The seeding concentration was optimized to give the maximum number of particles without supersaturating the liquid as well as yielding a high statistical correlation (i.e. a high signal to noise ratio) of the particle displacements within each interrogation zone for DPIV. The laser beam was expanded into a 40 mm wide and 1 mm thick laser sheet at the control volume using a plano-concave lens (focal length = −50 mm) in parallel with a positive cylindrical lens (focal length = 150 mm). The camera has a spatial resolution of 260×260 squared pixels and was configured to run at a frame rate close to 38 fps. The length of the sequences was 60 s, providing, on average, 2300 successive images that were captured digitally into Windows Bitmap images for further processing. A MATLAB code using the cross-correlation technique of two successive images has been utilized to process the data. The code locates the first and second peaks in the cross-correlation matrix and then uses a Gaussian function fitting in order to evaluate the sub-pixel velocity. In all the experiments, the camera was directed towards an area located above the top of the cylinder. The size of that area was 16 mm × 16 mm and has been kept constant for all tests. Care was taken to maintain the tank in a stable horizontal position during all experiments, i.e. to provide vibration isolation from other equipment in the laboratory.

3. Heat transfer characteristics around the cylinder

3.1. Calibration of the heat flux sensor

In addition to that carried out by the manufacturer, another laboratory calibration of the heat flux sensor has been conducted. The calibration consisted of measuring the heat flux at the cylinder surface for different circumferential positions of the sensor (achieved by rotating the cylinder around its axis) and for different Rayleigh numbers. The Rayleigh number was varied either by changing the temperature of the cylinder surface or by conducting tests in different fluids (air and water). When water is used, the free surface was at a distance of 250 mm from the cylinder. Preliminary experiments showed that this distance is large enough to neglect any effect of the free surface on the natural convection flow. For each experiment, the profile of

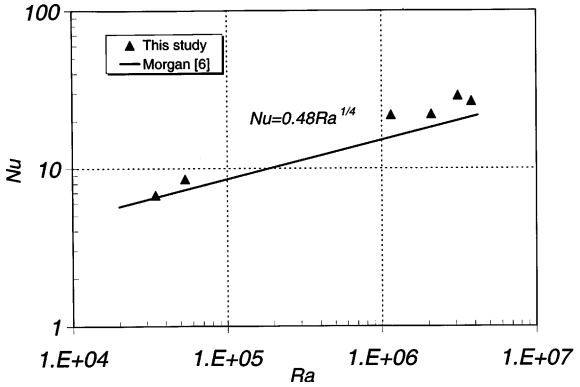

Fig. 2. Time-averaged Nusselt numbers against Rayleigh number compared with the empirical correlation of Morgan [6].

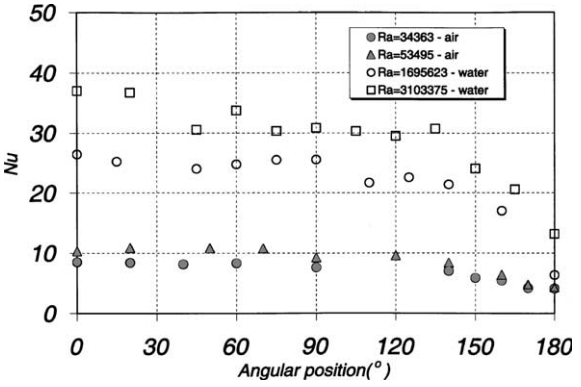

Fig. 3. Profiles of the local Nusselt number as a function of the angular position for different Rayleigh numbers.

local heat fluxes around the cylinder has been measured. The corresponding local Nusselt number has been computed for each heat flux as well as the average Nusselt number around the cylinder. Fig. 2 depicts the variation of the average Nusselt number (Nu) as a function of the Rayleigh number (Ra). Morgan [6] compiled datasets for natural convection around a heated cylinder in unbounded fluid media from different authors and came up with a correlation valid for a Rayleigh number ranging from 10^4 to 10^7. The correlation proposed by Morgan is plotted in the same figure. It can be seen that our experimental data are consistent with the empirical correlation.

3.2. Local heat flux profiles

The variation of the local Nusselt number as a function of the angular position around the cylinder is presented here for a range of Rayleigh numbers. In this set of experiments, the cylinder was not bound in the vertical direction; thus, for the tests in water, the water level was distant from the cylinder.

Fig. 3 shows the local profiles of the Nusselt number (Nu) measured at four different Rayleigh numbers (Ra). As expected, the heat transfer is higher on the lower part of the cylinder ($\beta = 0°$) in all cases. For the three lowest Rayleigh numbers, the same trend is observed; the graph is flat for all positions up to an angle of $\beta \sim 100°$, following which it decreases over the upper part of the cylinder. For the highest Rayleigh number, the decrease in Nusselt number is almost continuous from $\beta = 0°$ to $\beta = 180°$. Kreith and Bohn [7] indicated, in a review of empirical correlations for natural convection around a cylinder, that the heat flux (therefore the local Nu) decreases with the angular position. However, these authors did not mention any dependence of the trend on the Rayleigh number.

3.3. Effect of vertical confinement on heat transfer

In this section, the effect of vertical confinement is examined, using data obtained with water as a test fluid. In order to gain preliminary insight, two extreme water levels were investigated first: $H/D = 1/5$ and $H/D = 4$. Fig. 4 shows the profiles of the local Nusselt number as a function of the angular position for these water levels. Despite the fact that the Rayleigh number is somewhat higher, the profile measured at $H/D = 1/5$ shows an average Nusselt number considerably lower than that measured for $H/D = 4$. The shape of the two profiles is similar but the ratio of the maximum to the minimum (measured respectively on the lower and upper parts of the cylinder) is different. Indeed, this ratio is around 2.4 for $H/D = 4$ whereas a value greater than 6 is measured in the other case.

The lower heat flux values observed for $H/D = 1/5$ can be explained by the decay in the temperature difference between the cylinder and the free surface re-

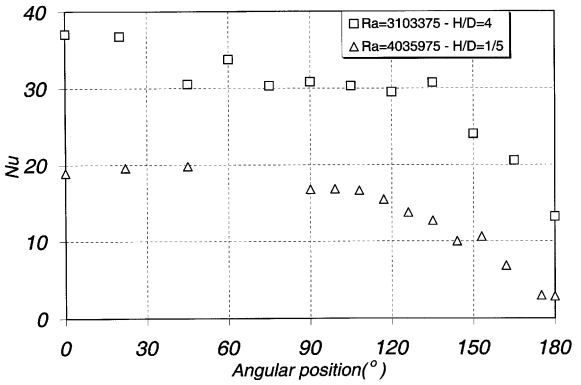

Fig. 4. Profiles of local Nusselt numbers measured in water for two different water heights.

corded throughout the experiment. Thus, the horizontal temperature difference used in the Rayleigh number calculation is unchanged but the local temperature difference falls due to the rise in temperature of the smaller volume of water above the heated cylinder. It is interesting to notice that this reduced local temperature difference affects the whole cylinder.

Similar experiments have been carried out for intermediate water levels, namely $H/D = 1$ and $H/D = 1/2$. The local Nusselt number profiles are shown in Fig. 5. The first point to note is that the average Nusselt numbers are comparable for Rayleigh numbers of the same order. However, the local variation in Nusselt number is significantly different from the steadily decreasing profiles of Fig. 4. At these intermediate water levels, the Nusselt number starts to increase at an angle $\beta \sim 150°$. For these two test conditions ($H/D = 1$ and $H/D = 1/2$), the Nusselt number on the upper part of the cylinder reaches values comparable to or higher than those measured on the lower part. It is interesting to notice that the increase is more pronounced for $H/D = 1$. In order to interpret the increase in heat flux on the upper part of the cylinder, time traces of the Nusselt number have been examined. Fig. 6 shows time

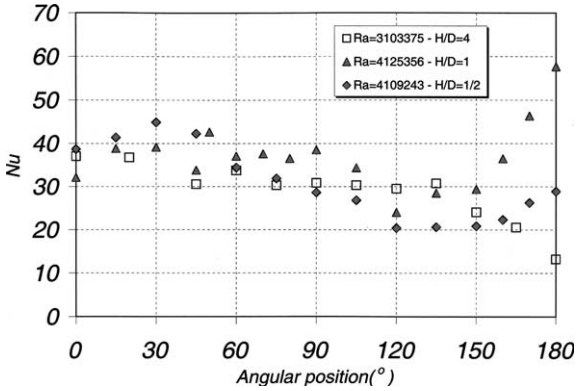

Fig. 5. Profiles of local Nusselt numbers measured in water for three different water heights.

varying Nusselt numbers recorded at two different locations: $\beta = 0°$ and $\beta = 180°$ for $H/D = 1/2$. The signal recorded at $\beta = 180°$ shows very low frequency oscillations around the mean, with the oscillations covering a range almost as large as the magnitude of the average Nusselt number (~30). Oscillations such as these have not been observed in the Nusselt number time traces

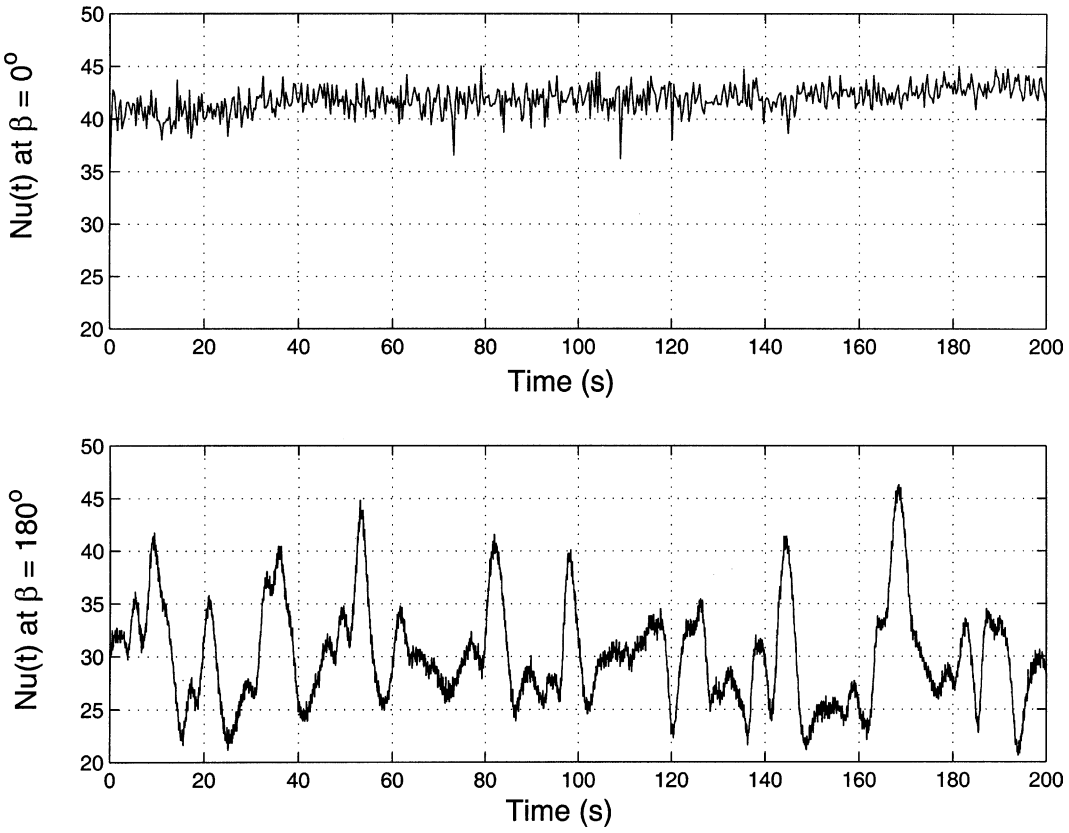

Fig. 6. Time series of the Nusselt number computed at two different positions for $H/D = 1/2$.

measured at $H/D = 1/5$ or $H/D = 4$. In the next section it will be shown that these oscillations are associated with an instability of the thermal plume above the cylinder. This instability makes the whole plume move from side to side, replacing the hot water close to the cylinder by fresh water, thereby increasing the flux.

4. Flow characteristics above the cylinder

Temporal and spatial variations of the vertical and horizontal velocity components in a plane area approximately 16 mm high and 16 mm wide located immediately above the cylinder have been measured using the DPIV technique. The plane area under investigation is normal to the axis of the cylinder. The results presented in this section have been obtained for three water heights: $H/D = 1/2$, $H/D = 1$ and $H/D = 3$. The velocity field for a water height $H = D/5$ has not been investigated as the heat transfer did not show any oscillatory character. These experiments have been carried out under similar thermal conditions, with a bulk water to cylinder temperature difference of $\Delta T = 15$ °C. The corresponding Rayleigh number is 6.3×10^6.

The first quantity to be examined is the velocity amplitude defined as:

$$A = \sqrt{U^2 + W^2}$$

where U and W are the horizontal and vertical velocity components respectively. Fig. 7 depicts the amplitude fields, for the three water heights, averaged over the duration of the experiments. The first point to note is that the shape of the regions with high velocity amplitudes is different in the three cases. For $H/D = 1/2$, the free surface effect is visible in the upper left part of the frame where, in addition to the main plume, a region with a relatively high velocity amplitude is observed. This high velocity amplitude region, a secondary vortex, moves downwards and is the result of the impact of the main plume against the free surface. In this particular case, the upper limit of the zone being viewed corresponds to the water surface. When the free surface is elevated to a height $H = D$ above the top of the cylinder, such a secondary vortex is not visible as the free surface is now half a diameter above the viewing zone. However, it is clear that the width of the plume has increased. When the free surface is elevated further to $H = 3D$, the shape of the plume is radically different from the previous ones. Indeed, the plume is narrower and the highest velocity amplitudes are located close to the top of the frame as opposed to the previous cases where the maximum velocity was positioned close to the middle of the frame. The differences in the maximum locations are the direct result of the presence of the free surface and the damping effect associated with it. When the water surface is positioned higher than $H = 3D$, the shape of the plume does not seem to change.

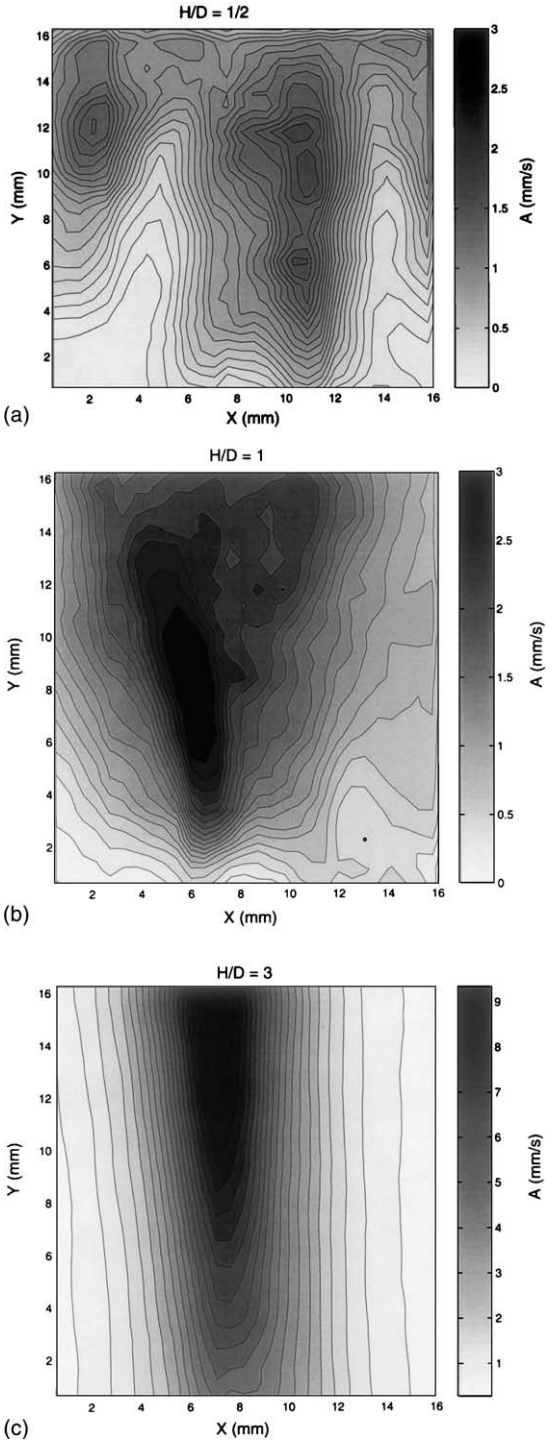

Fig. 7. Time-averaged velocity amplitude fields measured for three different water heights.

In order to compare the evolution of the velocity amplitude for the three water levels, Fig. 8 contains the horizontal profiles of this quantity measured at a distance $3/4H$ above the top of the cylinder. The profiles shown in this figure are time-averaged profiles. For the profile measured with a water level at $H/D = 1/2$, we observe that the maximum, located slightly off the image vertical axis, is accompanied by two local maxima at the sides. These two lateral peaks originate from the counter flow created by the plume impinging against the free surface. The two side peaks disappear when $H/D = 1$, for which case the maximum velocity amplitude is roughly twice that measured in the previous case. For $H/D = 3$, the profile is typical of a jet flow: symmetric around the center, and decreasing towards zero at the sides. The maximum in this case is 4 times higher than that recorded at $H/D = 1/2$.

It is interesting to look at the reasons why the plume is wider in the second case, for $H/D = 1$. To this end, a frame-by-frame analysis of the velocity amplitude field has been performed for the case where $H/D = 1$. Fig. 9 shows snapshots of the instantaneous velocity amplitude fields above the cylinder. The times at which the velocity is measured are reported at the top of each frame. We clearly see in this sequence that the plume, oriented

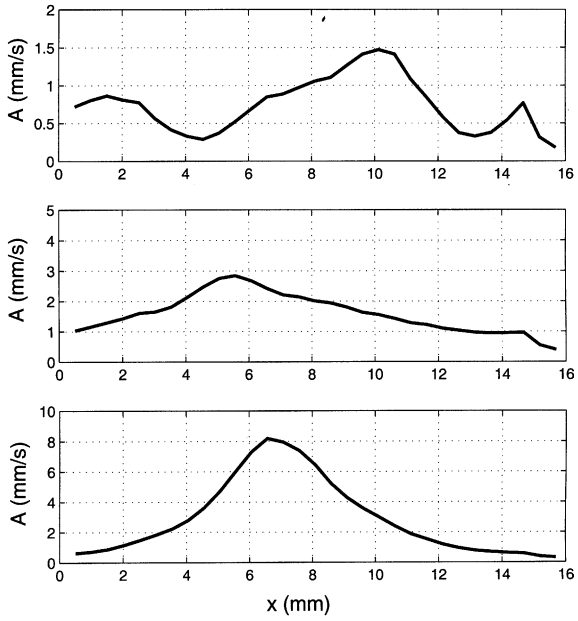

Fig. 8. Horizontal profiles of the velocity amplitude measured for three different water levels at a distance $h = 3H/4$.

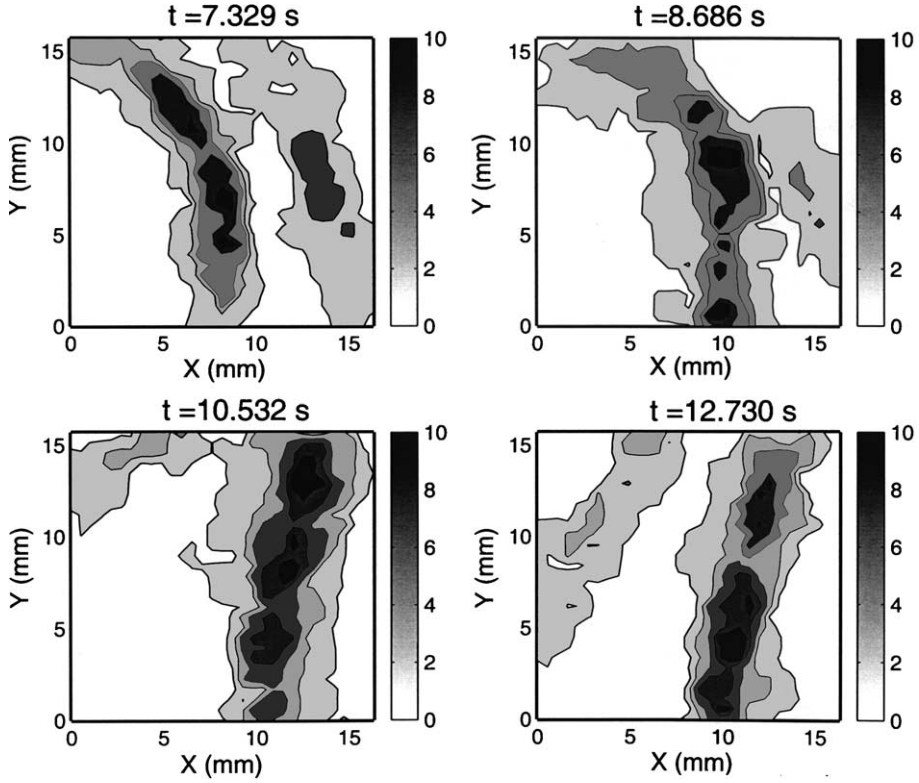

Fig. 9. Velocity amplitude snapshots measured at four different times during the same experiment for $H/D = 1$.

initially towards the left, moves slowly towards the center of the frame, and then goes to the far right. The time taken by the plume to move from left to right is very slow, more than 5 s. This time is different from that taken by the plume to go back to its initial position. Indeed, it takes the plume roughly 20 s to complete a total cycle. The same analysis has been done for the case where $H/D = 1/2$ and similar oscillations of the plume, with slightly higher oscillation frequencies, have been observed. However, the amplitude of the oscillations was lower. Such lower oscillation amplitudes explain the difference in heat flux enhancement between the cases where $H/D = 1/2$ and $H/D = 1$. They also explain the narrower plume observed in the first case.

In order to compare the plume motion in the three cases, we show in Figs. 10 and 11 respectively the horizontal and vertical velocity time series recorded at a height $0.9H$ on the vertical axis passing through the cylinder center. In each figure are reported the relevant velocities for the three cases as well as the water height.

The horizontal component of the velocity shows, as expected, large variations as a function of time for the two first cases. For its part, where the free water surface is far from the cylinder ($H/D = 3$ or higher), the horizontal velocity shows little or no fluctuations. The nature of the horizontal velocity fluctuations in the cases $H/D = 1/2$ and $H/D = 1$ are somewhat different. Thus, we observe that the horizontal velocity has a significant sine/cosine component for $H/D = 1$, with a period of 20 s. The negative and positive fluctuations are equal in magnitude (around -5 and 5 mm/s). For $H/D = 1/2$, this symmetry is not found. Indeed, the velocity tends to be close to zero for most of the time (meaning that the plume is stationary), and from time to time, the plume moves quickly to the left (negative velocity) or to the right (positive velocity). These intermittent plume motions are faster than those described for the case where $H/D = 1$.

The vertical velocity components shown in Fig. 11 lead to similar conclusions. Thus, this component is

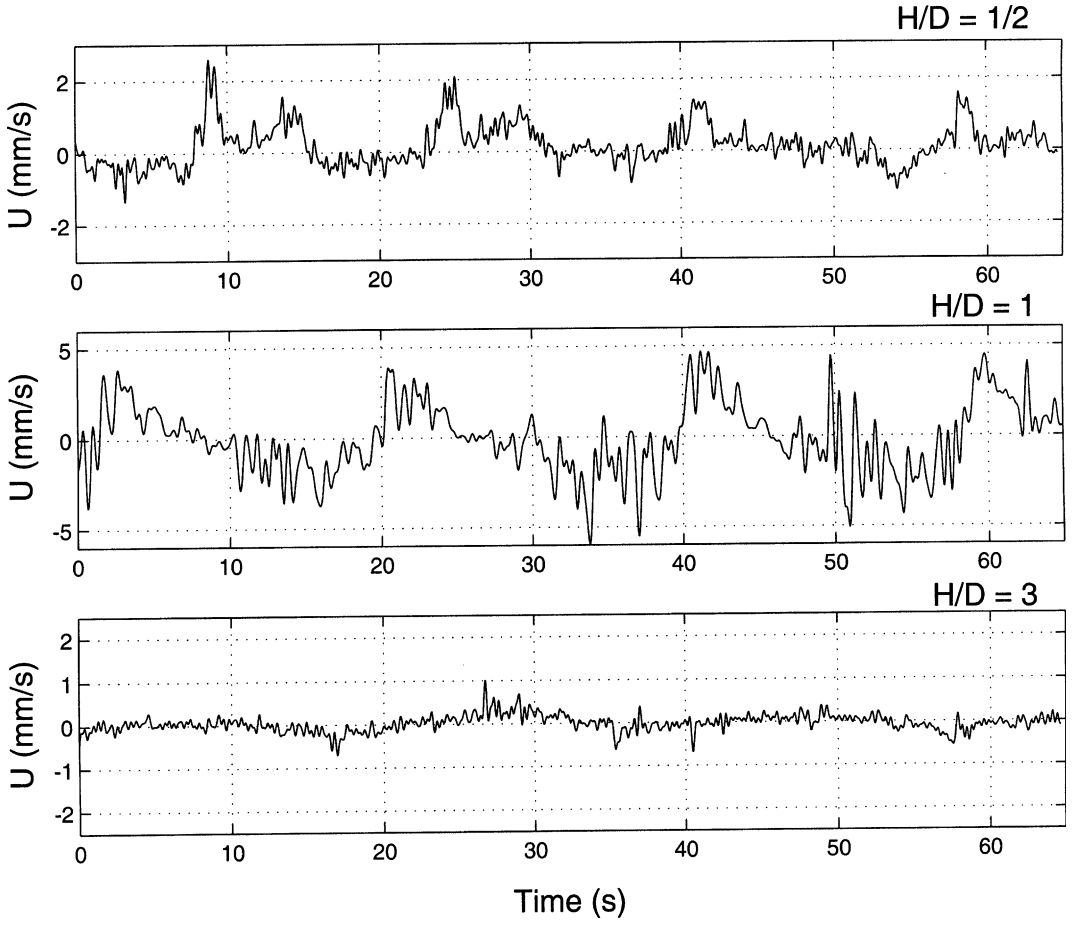

Fig. 10. Horizontal velocity time series measured for three different water heights at a distance $h = 0.9D$.

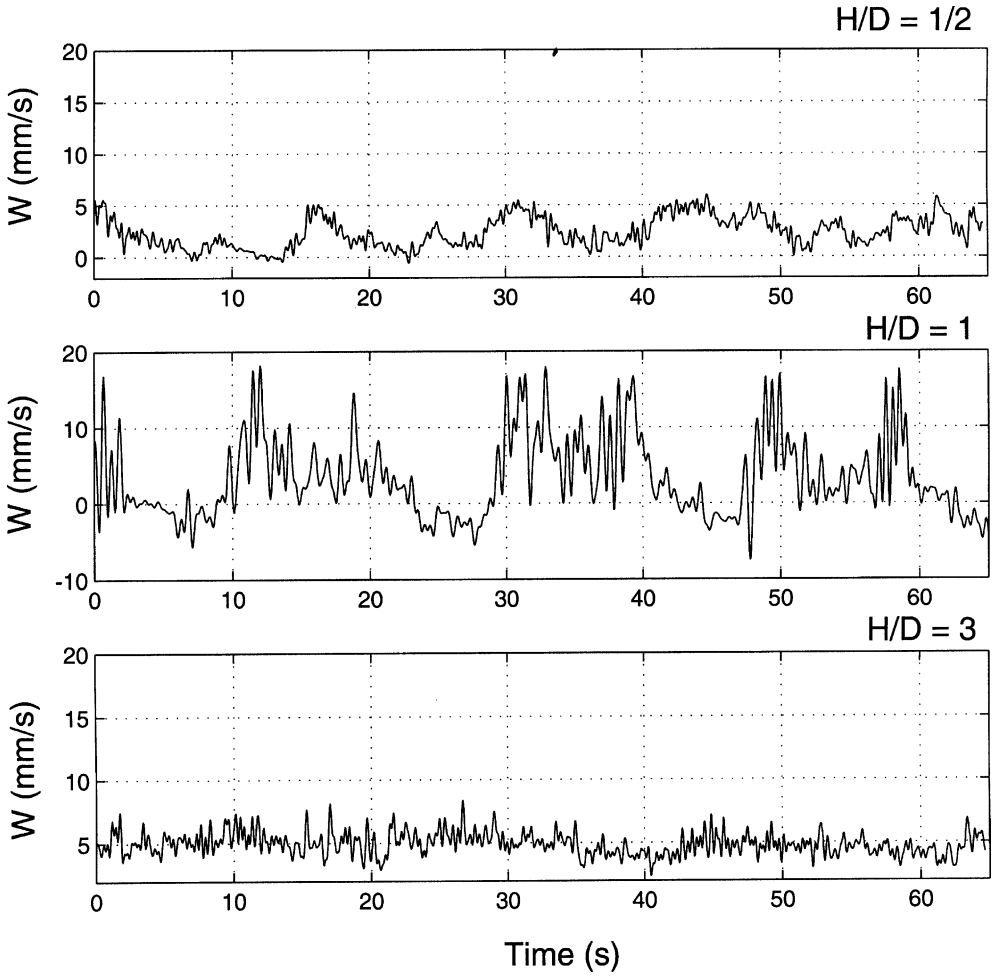

Fig. 11. Vertical velocity time series measured for three different water heights at a distance $h = 0.9D$.

relatively constant for the case where $H/D = 3$, indicating a stable plume. The fluctuations are low in frequency but large in amplitude for $H/D = 1$, and are faster and lower in magnitude for $H/D = 1/2$. The time series recorded for $H/D = 1$ gives an indication of how slowly the plume moves from one side to another. Thus, if we consider that the vertical velocity is close to zero when the plume is to one side, the time taken to move to the other side is the time between two successive zeros. That time interval is typically between 15 and 20 s.

The origins of the plume oscillation are not totally clear. Amongst other possibilities, one can consider the interactions between the secondary vortices above the cylinder and the free surface. The existence of two vortices, one at each side of the plume, is an unstable situation. Liu and Tao [8] investigated such a situation in a natural convection flow above two vertical heated plates mounted one parallel to the other. The flow was vertically bound by a ceiling. These authors simulated numerically the flow and observed large-scale oscillation where the oscillation periods were Rayleigh number dependent. The similarity with the current flow consists in the way the vortices generated below the ceiling gave rise to oscillations underneath them, in between the two parallel plates. In the present case, the instability leading to the oscillation at the cylinder level originates from a differential horizontal movement of one of the secondary vortices (with respect to the other) at the free surface. The displacement of these vortices induces the movement of the vertical plume to one side or another and, therefore, triggers the oscillation at the top of the plume. Such an instability is supported by the visualizations of Koizumi and Hosokawa [4]. It is not clear from our data how the instability of the vortices arises. One possible explanation could be the asymmetry of the temperature distribution at the free surface. Such an asymmetry creates an unbalance in the buoyancy forces, drives the thermal plume to one side and starts the oscillatory

cycle. However, a strict evidence to support this scenario cannot be presented here. Such evidence necessitates measurements of the local instantaneous temperature at various locations at the free surface.

5. Relationship between heat transfer and hydrodynamics

In order to have a better understanding of the relationship that exists between the velocity oscillations and the heat transfer quantities measured at the cylinder surface, a series of experiments has been carried out where the velocity field has been measured simultaneously with the heat transfer characteristics. The difference in temperature between the cylinder surface and the water bulk is $\Delta T = 15$ °C and the corresponding Rayleigh number is 6×10^6. The distance between the water level and the top of the cylinder was equal to one diameter of the cylinder ($H/D = 1$). The temperature was measured at the surface of the cylinder and below the free surface, on the vertical line through the center of the cylinder. The temperature and heat flux sensors and the DPIV acquisition systems have been connected to an external trigger so that the start of the acquisition on both systems is synchronized.

Fig. 12 is a plot of the Nusselt number time series ($Nu(t)$) together with the vertical component of velocity recorded at $D/6$, $D/3$ and $D/2$. The vertical velocity time series recorded at the three positions shows many similarities with the heat flux recorded at the cylinder surface. Thus, during the first 20 s, the Nusselt number rises and falls twice from less than 50 to more than 60. During the same time interval, the vertical velocity component exhibits similar behavior (from 0 mm/s to more than 10 mm/s). This trend can be observed throughout the experiment. However, some differences can be noticed between the time series. For instance, the variations in $Nu(t)$ become irregular (in terms of peri-

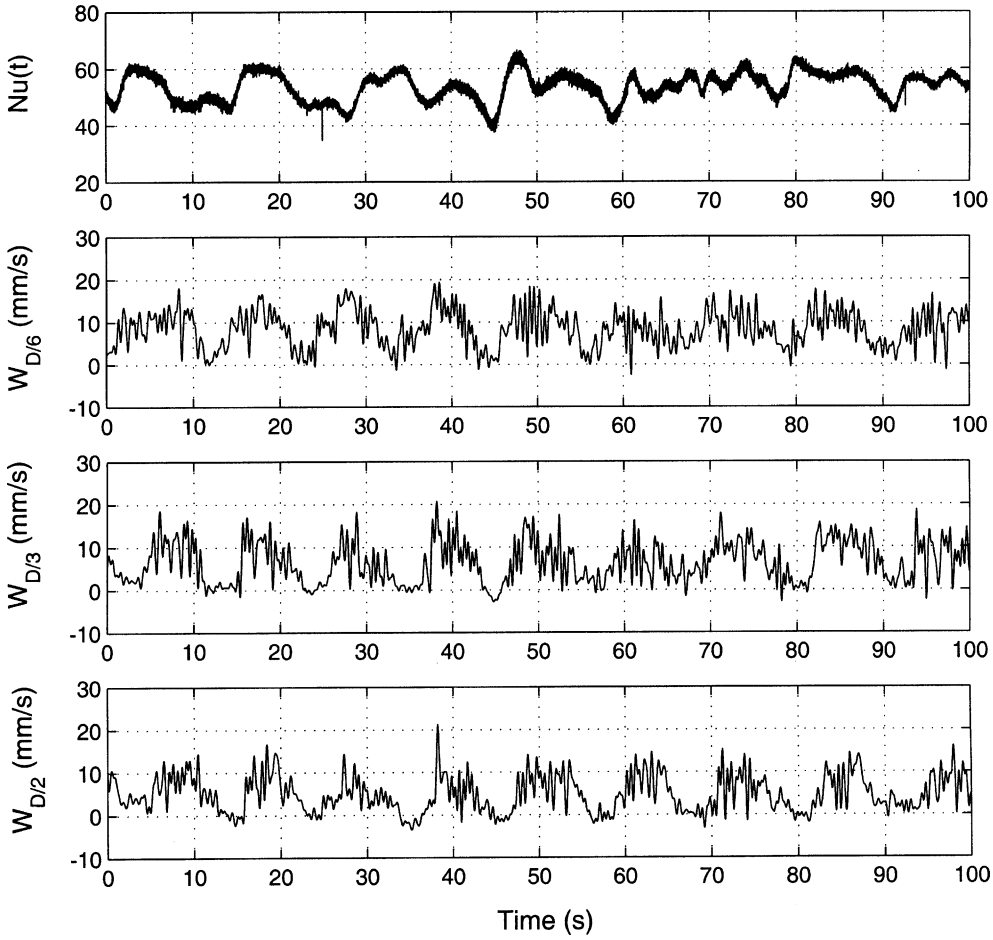

Fig. 12. Vertical velocity time series measured at three different positions along the same axis and the simultaneous heat flux time series measured at the surface of the cylinder.

odicity) at a time $t = 60$ s. That is not observed in the velocity time trace. It is likely that these differences originate from the fact that the two sets of time traces are not measured at the same location. Indeed, the DPIV measurement point at $D/6$ is located 5 mm above the cylinder top. That means that fast, small-scale motion of water very close to the surface of the cylinder is not likely to be captured by the DPIV system as set up here. The velocity time series recorded at the three positions show a similar behavior, with the only difference to be observed being in the amplitude of those velocities.

In order to confirm this difference in time scales between the quantities recorded at the cylinder and those in the fluid, the time series of the temperatures measured respectively at the surface of the cylinder and just below the free water surface are plotted in Fig. 13. Here again, we observe that both time traces are dominated by large-scale oscillations. The difference resides in the number of peaks observed in the two time series. Thus, the number of temperature peaks measured below the water surface is three, corresponding roughly to a period of 15 s. The number of temperature peaks is higher at the surface of the cylinder, corresponding to shorter periods, roughly about 5 s.

Overall, these remarks confirm that a strong relationship exists between the movement of the plume and the enhancement of surface heat flux at the cylinder. However, it can be stated that the large-scale dynamics that control the plume far from the cylinder differs somewhat from the flow characteristics close to it. One way to explain this comes from closer inspection of the plume oscillations. Thus, it has been observed that when the plume moves to one side, it does not stay in the same position but undergoes small amplitude oscillations about its new, mean position. Such secondary movement, although not significant when viewing the plume oscillation, can have important effects at the surface of the cylinder.

In their experiments, Koizumi and Hosokawa [4] carried out an analysis of the time varying heat flux in a configuration similar to that investigated here. The experimental differences were in the boundary conditions

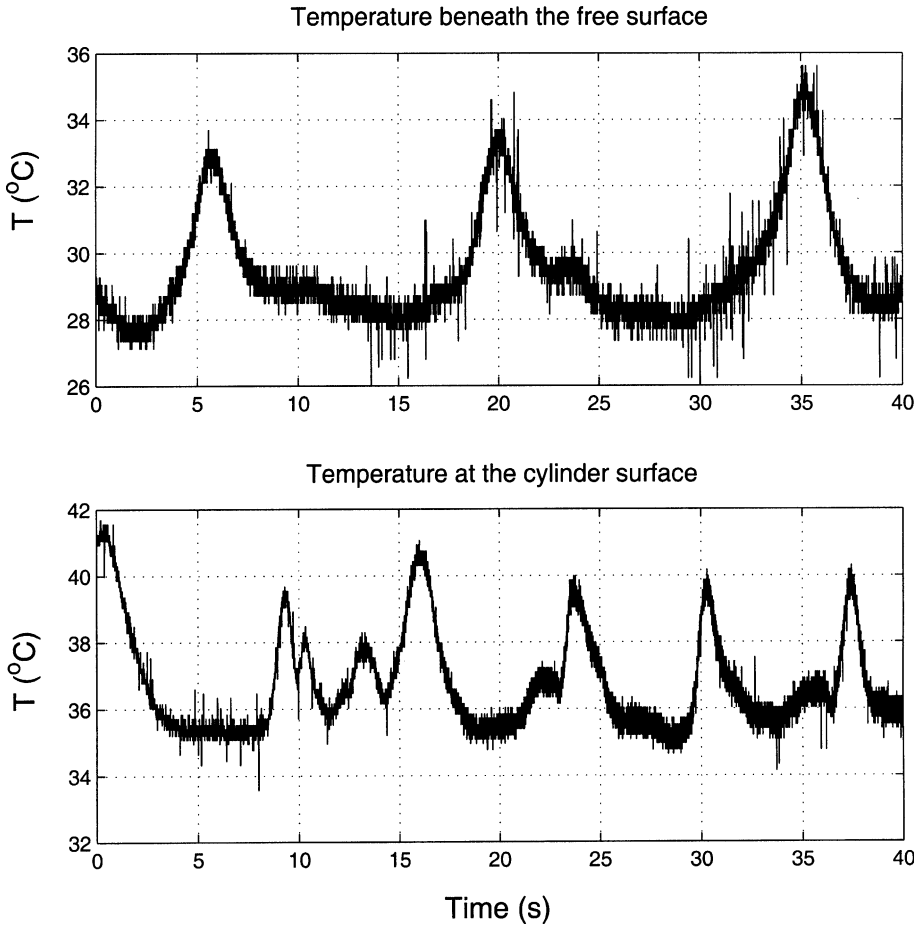

Fig. 13. Temperature time series measured at the surface of the cylinder and below the free surface.

they imposed in place of the water surface used here. Thus, their tests were conducted with air as a fluid medium and with both a constant temperature ceiling and an adiabatic ceiling. These authors also presented a diagram in which it is mentioned that for a flow similar to that investigated here ($Ra = 6 \times 10^6$ and $H/D = 1$), the thermal plume has a strong 3-D oscillatory and chaotic behavior. Small-scale oscillations with periods of 2 s or less were reported in that study, which is an order of magnitude smaller than the periods measured here. However, it is not clear if these periods are associated with the chaotic small scales or oscillatory large scales. A quantitative comparison with our results cannot be made.

6. Conclusion

Vertical confinement of the natural convection flow above a heated horizontal cylinder has been investigated. It has been shown that conducting such experiments in water with a free surface close to the cylinder can increase the heat flux from the top of the cylinder. However, for a very small cylinder to free surface separation (case where $H/D = 1/5$), the Nusselt number around the cylinder is dramatically reduced.

Investigation of the heat flux time series at the top of the cylinder indicated the presence of large scale, near periodic oscillations of the heat flux and temperature recorded at the cylinder surface. These oscillations have been further investigated using the DPIV technique. The hydrodynamics fields showed that the thermal plume is not stable and moves from one side of the vertical axis of the cylinder to another.

The relationship between the oscillations in the cylinder heat transfer characteristics and the hydrodynamics has been investigated. In particular, it has been shown that surface heat transfer at the cylinder oscillates more rapidly than the global movement of the plume. These differences originate from the secondary movement of the thermal plume when it is positioned at one side or another of the vertical axis through the cylinder center.

This work shows that, for a Rayleigh number of the order of 6×10^6, the natural convection flow around a heated cylinder, vertically bounded by a free surface, can undergo a transition from stable to unstable when the distance between the free surface and the cylinder is roughly equal to the diameter of the cylinder. This instability seems to disappear for low and large distances as the heat transfer results for $H/D = 1/5$ and $H/D = 3$ suggest.

Acknowledgements

The authors would like to thank G. Byrne from the mechanical engineering department at Trinity College Dublin for his help throughout this work.

Financial support for this work was provided by the Basic Research Program of Enterprise Ireland, under research grant no. SC/1998/711. The DPIV measurements were supported by the E.U. Development Host Fellowship scheme.

References

[1] K. Kitamura, F. Kami-iwa, T. Misumi, Heat transfer and fluid flow of natural convection around large horizontal cylinders, Int. J. Heat Mass Transfer 42 (22) (1999) 4093–4106.

[2] F. Karim, B. Farouk, I. Namer, Natural convection heat transfer from a horizontal cylinder between vertical confining adiabatic walls, J. Heat Transfer 108 (1986) 291–298.

[3] G. Cesini, M. Paroncini, G. Cortella, M. Manzan, Natural convection from a horizontal cylinder in a rectangular cavity, Int. J. Heat Mass Transfer 42 (10) (1999) 1801–1811.

[4] H. Koizumi, I. Hosokawa, Chaotic behavior and heat transfer performance of the natural convection around a hot horizontal cylinder affected by a flat ceiling, Int. J. Heat Mass Transfer 39 (5) (1996) 1081–1091.

[5] D.B. Murray, Local enhancement of heat transfer in particulate cross flow II—Experimental data and predicted trends, Int. J. Multiphase Flow 20 (3) (1994) 505–513.

[6] V.T. Morgan, The overall convective heat transfer from smooth circular cylinder, in: Irvine, Hartnett (Eds.), Advances in Heat Transfer, Academic Press, New York, 1975, pp. 199–264.

[7] F. Kreith, M.S. Bohn, Principles of Heat Transfer, fifth ed., Boston PWS Pub, 1997.

[8] J.P. Liu, W.Q. Tao, Bifurcation to oscillatory flow of the natural convection around a vertical channel in rectangular enclosure, Int. J. Numer. Methods Heat Fluid Flow 9 (2) (1999) 70–185.